Neuropsychologia 163 (2021) 108064

Contents lists available at ScienceDirect

Neuropsychologia

journal homepage: www.elsevier.com/locate/neuropsychologia

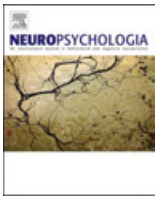

Neural responses to reflection symmetry for shapes defined by binocular disparity, and for shapes perceived as regions of background

Elena Karakashevska [a], Giulia Rampone [a], John Tyson-Carr [a], Alexis D.J. Makin [a], Marco Bertamini [a,b,*]

[a] University of Liverpool, Department of Psychological Sciences, Eleanor Rathbone Building, University of Liverpool, Liverpool, L69 7ZA, United Kingdom
[b] Department of General Psychology, Via Venezia, 8 – 35131, University of Padova, Padova, Italy

ARTICLE INFO

Keywords:
Symmetry
EEG
Perception
Stereopsis
SPN
Depth perception

ABSTRACT

Human perception of symmetry is associated with activation in an extended network of extrastriate visual areas. This activation generates an ERP called the Sustained Posterior Negativity (SPN). In most studies so far, the stimuli have been defined by luminance. We tested whether the SPN is present when stimuli are defined by stereoscopic disparity using random dot stereograms (RDS). In *Experiment 1*, we compared the SPN signal for contours specified by binocular disparity and contours specified by monocular cues. The SPN was equivalent, suggesting that the type of contour does not alter the SPN signal. In *Experiment 2* we exploited the unique property of RDS to provide unambiguous figure-ground arrangements. Psychophysical work has shown that symmetry is more easily detected when it is a property of a single object (i.e., within a figure), compared to a property of a gap between two objects (i.e., the ground). Therefore, the target regions in this experiment could either be foreground or background. The SPN onset was delayed when the symmetry was in a ground region. This may be because object formation interferes with the processing of shape information in the ground region.

1. Introduction

The visual system organises images projected on the retina into coherent scenes, a crucial step in perceptual organisation and figure-ground segmentation. Extensive work has been done on the rules which govern perceptual organisation (Wagemans et al., 2012). Fundamental cues include symmetry, convexity and closure.

The human visual system is extremely sensitive to symmetry. Studies have shown that the detection of symmetry is fast, accurate, and robust. Symmetry detection happens efficiently even with brief presentations (Carmody et al., 1977; Barlow and Reeves, 1979) and with peripheral presentation (Barlow and Reeves, 1979; Rampone et al., 2016). Symmetry in 2D refers to self-similarity under rigid transformations. Although rotation and repetition are possible transformations, mirror reflection is the most salient for human observers (Mach, 1897), and perhaps the most biologically relevant (Little et al., 2011). Symmetrical 3D objects only project a symmetrical 2D image when observed from a non-generic viewpoint (Swaddle, 1999; Szlyk et al., 1995, Chen et al., 2007). Affine and perspective transformations (Makin et al., 2015; Sawada and Pizlo, 2008; Wagemans et al., 1991) do not abolish symmetry perception, although they can be disruptive. In the current study we focus on brain responses to 3D images with both vertical and horizontal axes of reflection.

The neural response to visual symmetry has been extensively studied in the last two decades (Bertamini et al., 2018; Bertamini and Makin, 2014; Cattaneo, 2017). An EEG study by Norcia et al. (2002) reported that symmetry selectivity emerges about 220 ms after stimulus onset. Further ERP studies have consistently reported negative amplitude at posterior electrodes when participants view symmetrical patterns (Jacobsen & Höfel, 2003, 2003, 2003; Makin et al., 2012a,b; Martinovic et al., 2018). This ERP signal has been termed the Sustained Posterior Negativity (SPN). The SPN is a relative measure, given by the difference between symmetry and asymmetry waves. The SPN can be recorded during active symmetry discrimination or during a secondary task (Höfel and Jacobsen, 2007; Jacobsen and Höfel, 2003; Makin et al., 2013). In addition, Palumbo et al. (2015) found a linear increase in SPN amplitude with the proportion of symmetrical elements in the display (see also Makin et al., 2020). Makin et al. (2016) reported that SPN

* Corresponding author. University of Liverpool, Department of Psychological Sciences, Eleanor Rathbone Building, University of Liverpool, Liverpool, L69 7ZA, United Kingdom.
E-mail address: m.bertamini@liverpool.ac.uk (M. Bertamini).

https://doi.org/10.1016/j.neuropsychologia.2021.108064
Received 22 March 2021; Received in revised form 13 October 2021; Accepted 15 October 2021
Available online 16 October 2021

amplitude closely correlates with perceptual goodness across a range of regularity types, including Glass patterns, repetition, and reflectional symmetry.

Source localization suggests that the SPN is generated by the extrastriate cortex (Kohler et al., 2016; Makin et al., 2012a,b). This is in line with functional MRI work which has found symmetry activation in a network of areas in the extrastriate cortex (V3, V3a, V4, and LOC), with the strongest responses in the shape-sensitive Lateral Occipital Complex (LOC) and V4 (Sasaki et al., 2005; Tyler et al., 2005). This is also consistent with Transcranial Magnetic Stimulation (TMS) studies, which have shown that the LOC plays a causal role in symmetry perception (Cattaneo et al., 2014).

To date, neuroimaging work has measured brain responses to symmetrical objects or patterns. However, it has not directly addressed the importance of symmetry in figure-ground segmentation. Several different psychophysical studies have suggested that symmetry processing is directly involved in the grouping and segmentation of visual input. Bahnsen (1928) was the first to illustrate the importance of symmetry as a cue for perceptual grouping. His subjects reported seeing regions with symmetric contours as figures with asymmetric ground spaces on 90% of the trials. However, Kanizsa and Gerbino (1976) found symmetry to be less powerful as a grouping factor when compared to convexity. More recently, Mojica and Peterson (2014) demonstrated that symmetry and convexity are equally effective cues, but symmetry plays a role in perceptual organisation only when it is close to fixation. Machilsen et al. (2009) used co-alignment in Gabor stimuli to explore the role of symmetry in object perception. Thresholds for detecting a shape in noisy displays were significantly lower for symmetrical shapes, indicating a role for symmetry in perceptual organisation.

Another line of research has explored the relative salience of symmetry when it is a property of an object compared to when it is a property of a region between two objects (i.e., in the ground). A common finding is that bilateral symmetric contours are more efficiently perceived when they belong to a single object compared to when they are between two different objects. For repetition this is reversed: repetition is more efficiently detected when the contours belong to two objects (Baylis and Driver, 1995; Bertamini et al., 1997, 2002; Corballis and Roldan, 1974; Koning and Wagemans, 2009; Makin et al., 2012a,b; Treder and van der Helm, 2007). A study by Treder and van der Helm (2007) showed that detection of symmetry (but not of repetition) is poor when the corresponding elements of symmetrical contours are placed on different planes (i.e., at different depths). This further supports the claim that bilateral symmetry is a cue for the presence of a single object.

2. Current study

Stereoscopic 3D shape processing involves a complex set of mechanisms in both dorsal and ventral streams (Neri, 2005; Orban et al., 2006; Parker, 2007). With respect to binocular disparity, almost all regions of the visual cortex contain neurons that respond to disparity (Parker, 2007). Several neurophysiological studies have shown early responses to disparity (DeAngelis and Newsome, 1999; Livingstone and Hubel, 1988) and a recent EEG study by Duan et al. (2021) showed disparity sensitive responsesarise 150 ms post stimulus presentation. Object processing areas in the inferotemporal cortex can respond to shape defined solely by early stereoscopic disparity cues (Gilaie-Dotan et al., 2002). However, it is less clear whether stereoscopic information modulates higher-level perceptual processing like symmetry perception. The SPN may differ in magnitude or in latency if the symmetrical stimulus is defined solely using binocular information (disparity-defined contours, also known as cyclopean contours). In these stimuli, symmetry information is absent at the monocular level.

Furthermore, cyclopean contours specified in a random-dot stereogram (RDS) allow for direct figure-ground manipulation. The same region can be seen as in front (figure) or behind (ground) (Julesz, 1986). The second issue we investigated was whether the SPN would be altered by the figure-ground status of symmetrical stimuli. One possibility is that the SPN is reduced, or even abolished, when regularity is represented by a gap between two surfaces, because the symmetry is now not a property of an object, and the contours of the ground region belong to the outer objects. This would be consistent with the findings from speeded discrimination tasks (Bertamini et al., 1997) where symmetrical gaps between surfaces are discriminated less efficiently that symmetrical objects (the reverse is true for repetition).

The current study recorded the SPN for disparity-defined stimuli. In the experiments, depth separation was the only information available to define the shape of objects in the critical conditions. Experiment 1 compared the SPN waves for three types of stimuli defined by: binocular disparity; monocular contrast; and disparity and contrast. We predicted a similar SPN for the binocular and monocular cue conditions, and an additive effect on the SPN of having the two cues in the combined condition. The relationship between bilateral symmetry and contour ownership was the focus of Experiment 2. Bilateral symmetry may produce a different SPN when it is the property of an object than when it is a gap between contours belonging to other objects (round).

We predicted that the SPN amplitude for contours in RDS will be large and like the SPN produced by contrast defined contours in both experiments (figure condition). In the ground condition of Experiment 2, we predicted a reduction in SPN amplitude, and a change in the sustained response (faster decay). These effects would suggest that symmetry and object representation are mutually supportive. These predictions were pre-registered (https://osf.io/zv5t2/).

3. Experiment 1: binocular disparity defined contours

Experiment 1 investigated whether symmetry defined by stereoscopic information produces an SPN. Participants judged whether the contours presented were symmetrical or asymmetrical. Contours were specified by binocular disparity, monocular contrast or both cues combined (Fig. 1). In all conditions, shape was specified at a suprathreshold level. The critical region containing information about the regularity was in the centre of the screen. The hypothesis was that disparity-defined contours produce an SPN of similar magnitude as contours defined by monocular cues. We included a combined condition (monocular + binocular) to see whether this combined wave is the additive result of the waves in the other two conditions.

4. Experiment 1 methods

4.1. Participants

Twenty-eight individuals took part in Experiment 1 (age 18–30, mean age = 19.6, 8 male, 0 left-handed). All participants had normal or corrected-to-normal vision. They were also screened for stereo acuity using a standard TNO test. Their stereo acuity varied between 30 and 120 arc sec. The TNO test has been shown to overestimate the stereopsis thresholds (Vancleef et al., 2017), however here it was used only as a screening tool, to confirm that participants were not stereo blind. TNO estimates are not included in the analysis. The study had local ethics committee approval and was carried out in accordance with the 2008 version of the declaration of Helsinki. All participants signed an informed consent form.

4.2. Apparatus

EEG data was recorded continuously from 64 scalp electrodes arranged by the international 10–20 system. We used the BioSemi active-two EEG system, sampling at 512 Hz. Stimuli were presented to participants on a 54.4 × 33.2 cm monitor. HEOG and VEOG were monitored online to check for unwanted blinks and eye movements. The distance from the screen was constrained with a chinrest at 57 cm. The images and presentation were programmed in Python using PsychoPy libraries

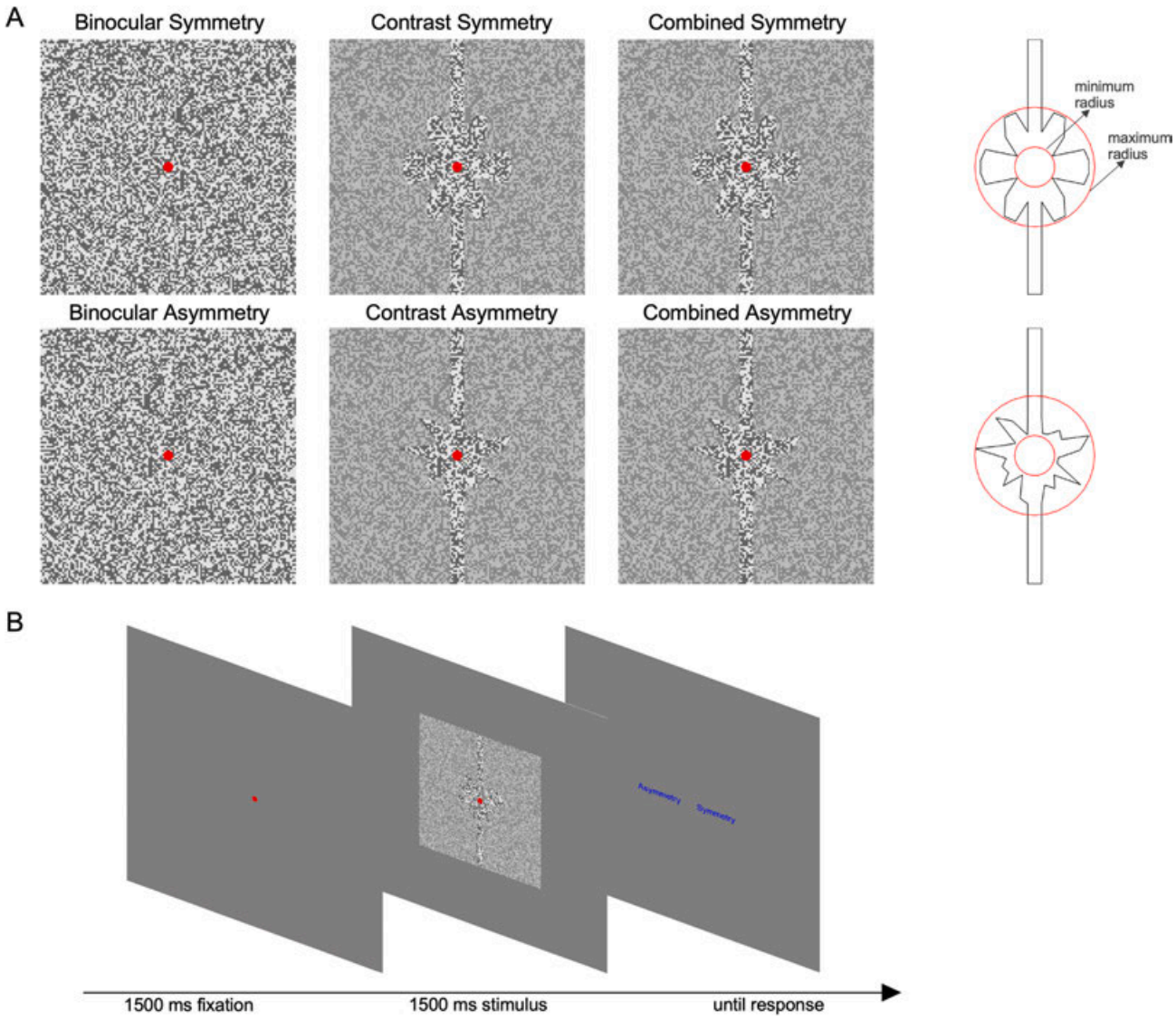

Fig. 1. Stimuli and procedure for Experiment 1. A) Example of stimuli in each of the six conditions: Symmetry defined by disparity, by contrast and by both disparity and contrast; Asymmetry defined by disparity, by contrast and by both. In the disparity condition, the shape can only be seen after fusion. In the experiment no polygonal shape was repeated in more than one trial. B) The sequence of images presented during a trial included a fixation, a stimulus, and a response screen.

(Peirce, 2007). The stereo monitor (SONY) used a passive stereo system and had a resolution of 1920 × 1080 pixels at 60 Hz. Because of the polarized glasses, the effective vertical resolution was halved (540 pixels). Passive stereo was preferred to shutter glasses to avoid any interference with the EEG recordings.

4.3. Stimuli

The stimuli were random dot stereograms with light and dark grey squares, presented on a grey background (as in Fig. 2). Each stimulus had a matrix of 128 × 128 squares, and a side of 13.5° of visual angle. Therefore, each square was approximately 0.1° wide. The background region had zero disparity and the stimulus always appeared on the front plane with a disparity of 0.06°. In the binocular condition the luminance of each square was chosen at random between 22.0 cd/m^2 to 125 cd/m^2 on our monitor. The Michelson contrast (or visibility) for this condition was 0.70. For the contrast and combined condition, the luminance of the background plane ranged from 98.0 cd/m^2 and 47.0 cd/m^2, giving approximately the same average luminance value, but reducing the contrast to 0.34. Background grey was set at 35 cd/m^2. The plane containing the critical contour and the background plane were matched in luminance in each condition. The average luminance in each condition was approximately 73 cd/m^2. Our stimuli had regions that differed in disparity and in contrast, but the luminance was only approximately matched.

A red fixation dot (radius 0.43°) was present in the centre of the screen during fixation and during stimulus presentation. In half of the trials the stimulus was an irregular polygon. In the other half it had vertical and horizontal reflectional symmetry. Two axes of reflection were used because of the larger neural response that is generated by the presence of two axes (Makin et al., 2016).

The symmetrical and asymmetrical polygons were generated starting from a standard circle with a 2.16° radius. Along this circle we randomly selected 28 vertices. For each vertex, the radius could take values between 1.08° (minimum radius) and 3.24° (maximum radius). Different vertices were selected in each trail and therefore no trial repeated images used before. Each vertex was equally spaced (360°/28) except that this position varied for each vertex randomly by ± 1°(to add variability).

4.4. Procedure

Participants completed a TNO test to assess their stereo acuity.

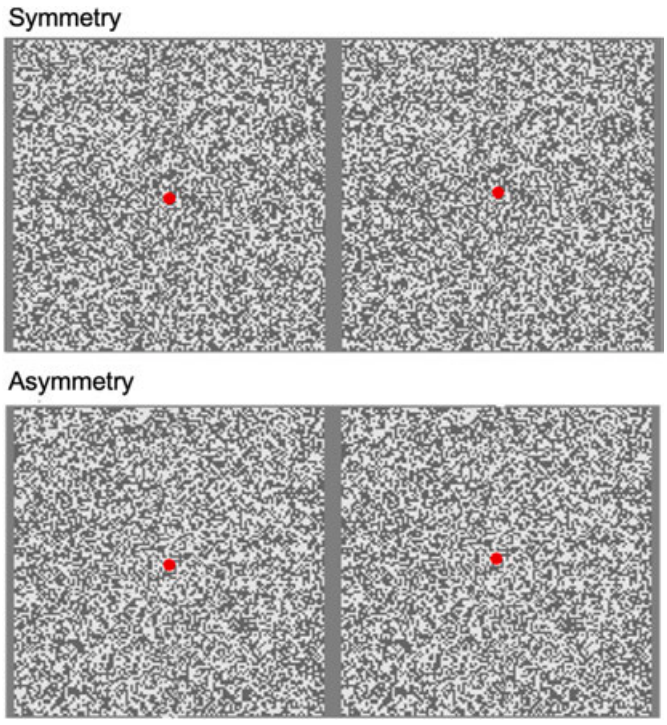

Fig. 2. Example of random dot stereograms for Experiment 1. The left image is for the left eye and the right image for the right eye. The disparity was increased from 0.06° to 0.23° for these examples.

Participants who scored above 120 arcsec were not tested. After the pre-screening, participants were fitted with the EEG cap and introduced to the EEG experiment. Participants initially completed a 40-trial practice block, identical to the main experiment except for the presence of an acoustic feedback for a wrong response.

Each trial began with 1.5 s of a red fixation dot. This was followed by a 1.5 s presentation of the stimulus. After the stimulus disappeared participants entered their responses using the keyboard without time pressure. Key mapping switched unpredictably on each trial. This is standard practice to avoid planning of motor responses during the stimulus presentation. The experiment consisted of 720 trials, split into 24 blocks. Condition trials were fully interleaved, each block contained an equal number of randomized trials of each condition. Thus, there were 120 trials in each condition: Symmetry (Symmetrical, Asymmetrical) X Contour (Disparity, Contrast, Combined) X Response screen (Left, Right).

4.5. ERP analysis

EEG analysis and pre-processing were based on previous EEG work on perception of symmetry (Makin et al., 2016). EEG data was recorded continuously and then processed offline using eeglab 13.4.4b (Delorme and Makeig, 2004) in Matlab. Data was first referenced to the scalp average, downsampled to 128 Hz, low pass filtered at 25Hz with the IIRFILT function, and then broken into epochs from −0.5 to +1.5 s around stimulus onset, with a −200 ms pre-stimulus baseline. Epoched data was cleaned with Independent Component Analysis (Jung et al., 2000). This process removed blink, movement, and other gross artefacts. An average of 17.18 components were removed from each participant (min = 6, max = 30). Trials where participants entered the incorrect response were removed. On average 2% of the trials were excluded per participant. After this, trials with amplitude more extreme than ±100 μV (μV) at any scalp electrode were excluded. The average overall exclusion rate was 8.3% for Binocular, 7.4% for Contrast and 6.1% for Combined. SPN was defined as the amplitude difference between symmetrical and asymmetrical conditions at the posterior electrode cluster [PO7 O1 O2 PO8] from 400 to 1500 ms post stimulus onset. The left [PO7 O1] and right pair [O2 PO8] from this cluster were used when comparing SPN across hemispheres. The electrodes were chosen a-priori, based on previous research. The SPN at these electrodes has been consistently associated with the extrastriate symmetry response and is a measure of persistent activation of the symmetry network (Makin et al., 2020).

5. Experiment 1 results and discussion

5.1. P1 and N1 analysis

Fig. 3A shows grand average ERP waves in each condition. The P1 was the same across both conditions, while N1 was larger in Binocular and Combined conditions. To explore P1 and N1, we obtained peak amplitude during the 100–180 ms and 180–260 ms time window, respectively. The time-windows for analysis were chosen based on previous studies looking at the effects of stereoscopic disparity on Visually Evoked Potentials (VEPs; Pegna et al., 2018). Peak amplitudes were analysed with mixed omnibus ANOVAs [3 Contour (Binocular, Contrast, Combined) X 2 Regularity (Symmetrical, Asymmetry) X 2 Hemisphere (Left, Right)]. There were no significant effects or interactions for P1 amplitude ($p > .213$). For N1, there was no main effect of Regularity ($F(1,27) = 0.77$, $p = .387$, $\eta_p^2 = 0.028$). However, there was a significant main effect of Hemisphere ($F(1,27) = 5.68$, $p = .024$, $\eta_p^2 = 0.174$) because N1 peak was reduced in the left hemisphere (mean = −0.39 μV, SD = 3.43) compared to the right hemisphere (mean = −1.67 μV, SD = 3.50). There was also a significant main effect of Contour ($F(2, 54) = 19.24$, $p < .001$, $\eta_p^2 = 0.416$). There was a significant difference between Contrast and Binocular ($t(27) = -4.666$, $p < .001$, dz = - 0.88) and Contrast and Combined ($t(27) = 4.352$ $p < .001$, dz = 0.82) conditions. There was no significant difference between Binocular and Combined conditions ($t(27) = -0.080$, $p = .937$, dz = 0.02). There were no significant interactions.

These results confirmed that the stereo manipulation in the experiment was sufficient to elicit an early response to the onset of the disparity defined shape. Our findings are in line with previous research examining the effects of stereo input on the VEPs. For instance, Oliver et al. (2018) showed that stereo viewing affects activation early in the visual stream.

5.2. SPN analysis

The SPN is defined as the difference between symmetry and asymmetry waves, see plot on the right in Fig. 3A. The plot on the right in Fig. 3B illustrates 95% Confidence intervals around these waves. When these cross zero, there is a significant SPN. For statistical analysis, the SPN was defined as the amplitude of the difference wave in the 400–1500 ms interval. Trials where participants pressed the wrong button were excluded from analysis. SPN amplitude on correct trials was examined with 3 × 2 ANOVA [3 Contour (Binocular, Contrast, Combined) X 2 Hemisphere (Left, Right)]. There was no main effect of Contour ($F(2, 54) = 0.30$, $p = .739$, $\eta_p^2 = 0.011$), therefore the SPN produced by disparity-defined contours does not differ from SPN produced by contrast-defined contours. There was no main effect of hemisphere ($F(1, 27) = 0.63$, $p = .434$, $\eta_p^2 = 0.023$) and no significant interactions. The average SPN was significant in each condition: Binocular (mean = - 0.56 μV, SD = 0.71, $t(27) = 4.174$, $p < .001$, dz = −0.79), Contrast (mean = - 0.65 μV, SD = 0.97, $t(27) = 3.565$, $p = .001$, dz = −0.67) and Combined (mean = - 0.70 μV, SD = 0.90, $t(27) = 4.266$, $p < .001$, dz = −0.81). These effects also illustrated with 95% CI in Fig. 3D.

Our findings indicate that the symmetry-sensitive ERP component is equivalent for contrast-defined and stereo-defined contours. Contour can be specified in different ways, and they are equivalent in terms of the symmetry response once a shape is clearly visible. Previous research has

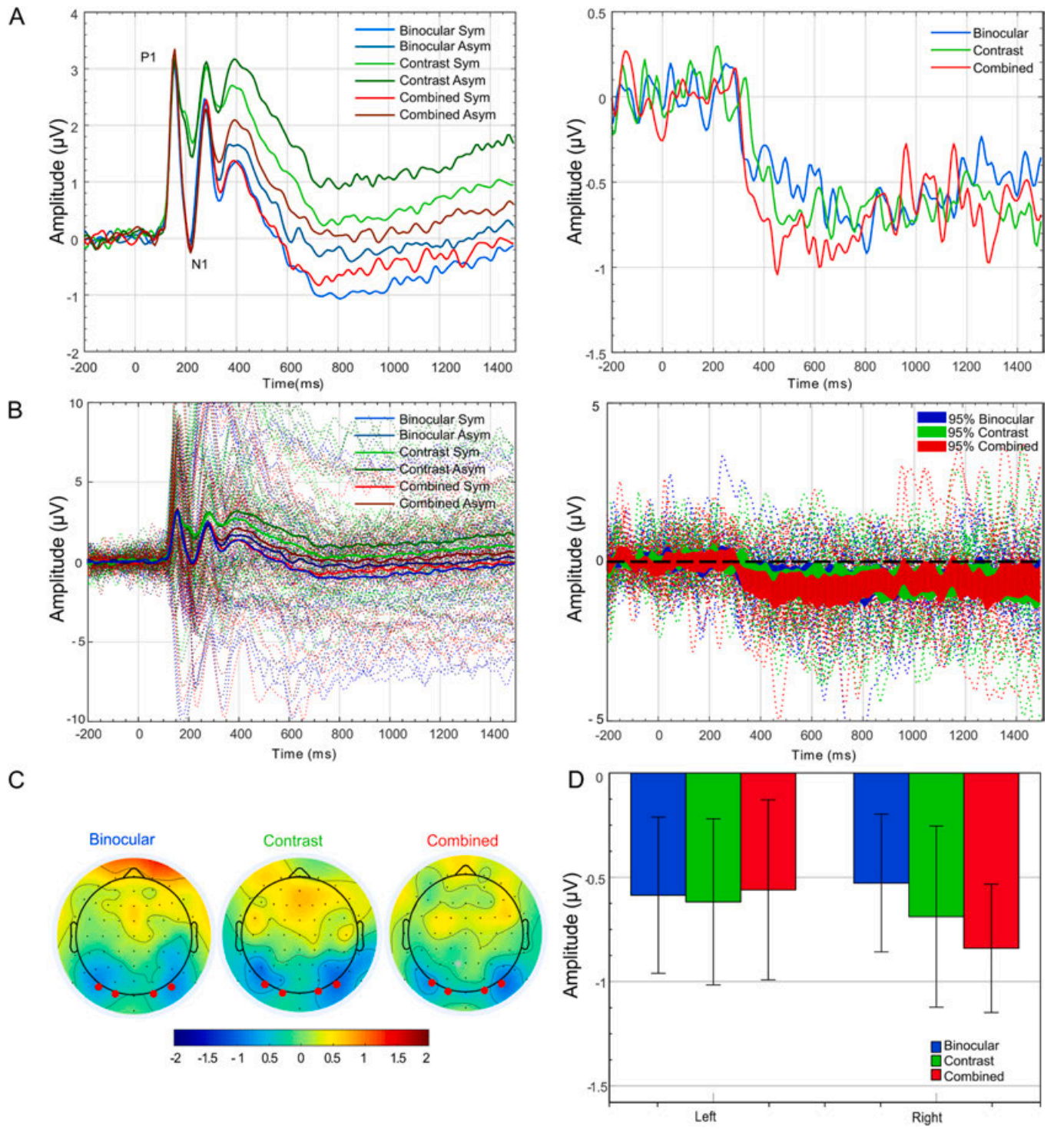

Fig. 3. A) Grand average ERPs and SPN difference waves for Experiment 1: Waves were taken from bilateral posterior electrode cluster [PO7 O1 O2 PO8] annotated in B. The first plot shows the average ERPs, and the second plot shows the SPN as a difference from the asymmetry wave. B) Inter-subject variability. These plots are similar to panel A but include visualization of inter-subject variability. The first plot shows individual-subject ERPs behind grand averages. The second plot shows 95% CI around the SPN as well as individual-subject SPNs. When the coloured ribbons do not cross zero, the SPN is significant. C) Topographic difference maps: These illustrate the difference between symmetrical and asymmetrical maps in a time window from 400 to 1500 ms for binocular, monocular and combined contours. Here the SPN appears as blue at posterior electrodes. D) SPN amplitudes: Bars show difference from asymmetry (500–1500 ms) in the three stimulus domains. Error bars = 95% confidence intervals. (For interpretation of the references to colour in this figure legend, the reader is referred to the Web version of this article.)

shown that at supra-threshold level, low and mid-level visual information contribute to symmetry perception (Bertamini et al., 2018). For instance, our results are consistent with Martinovic et al. (2018) who reported similar SPN for different supra-threshold luminance and colour defined symmetries. Symmetry perception is indifferent to low level properties of the symmetrically arranged elements.

The most important result from Experiment 1 is a null result: There was no significant difference in SPN amplitude across the three contour types. However traditional null hypothesis significance testing (NHST) cannot be used to confirm this. ANOVAs give the probability of

obtaining the observed data given the null hypothesis (pD|H0), not the probability of a null hypothesis being true given the observed data (pH0|D). We thus used Bayesian alternatives to NHST to estimate pH0|D (Masson, 2011), using the supplementary materials provided (for the workings see https://osf.io/zv5t2/). For the main effect of Contour, pH0|D = 0.964, and thus PH1|D = 1-0.964 = 0.036. This confirms that the evidence is a better fit to the null hypothesis, and the SPN was not influenced by contour type.

6. Experiment 2: figure-ground segmentation

A common finding in the psychophysical literature is that symmetry is more easily detected when it is a property of a single object than a gap between two objects (Baylis and Driver, 1995; Bertamini et al., 1997). In Experiment 2 we tested whether this influences the SPN. Participants judged whether the contours presented in the central region were symmetrical or asymmetrical. Contours were specified by binocular disparity only. The disparity levels were tested and were above threshold levels, therefore participants performed the task accurately. The central region contained information about regularity, but this region could be defined as foreground (a single surface) or background (a gap between two outside surfaces). Thus, because of unidirectional contour ownership, the contours could belong to the central region or to the two outside regions.

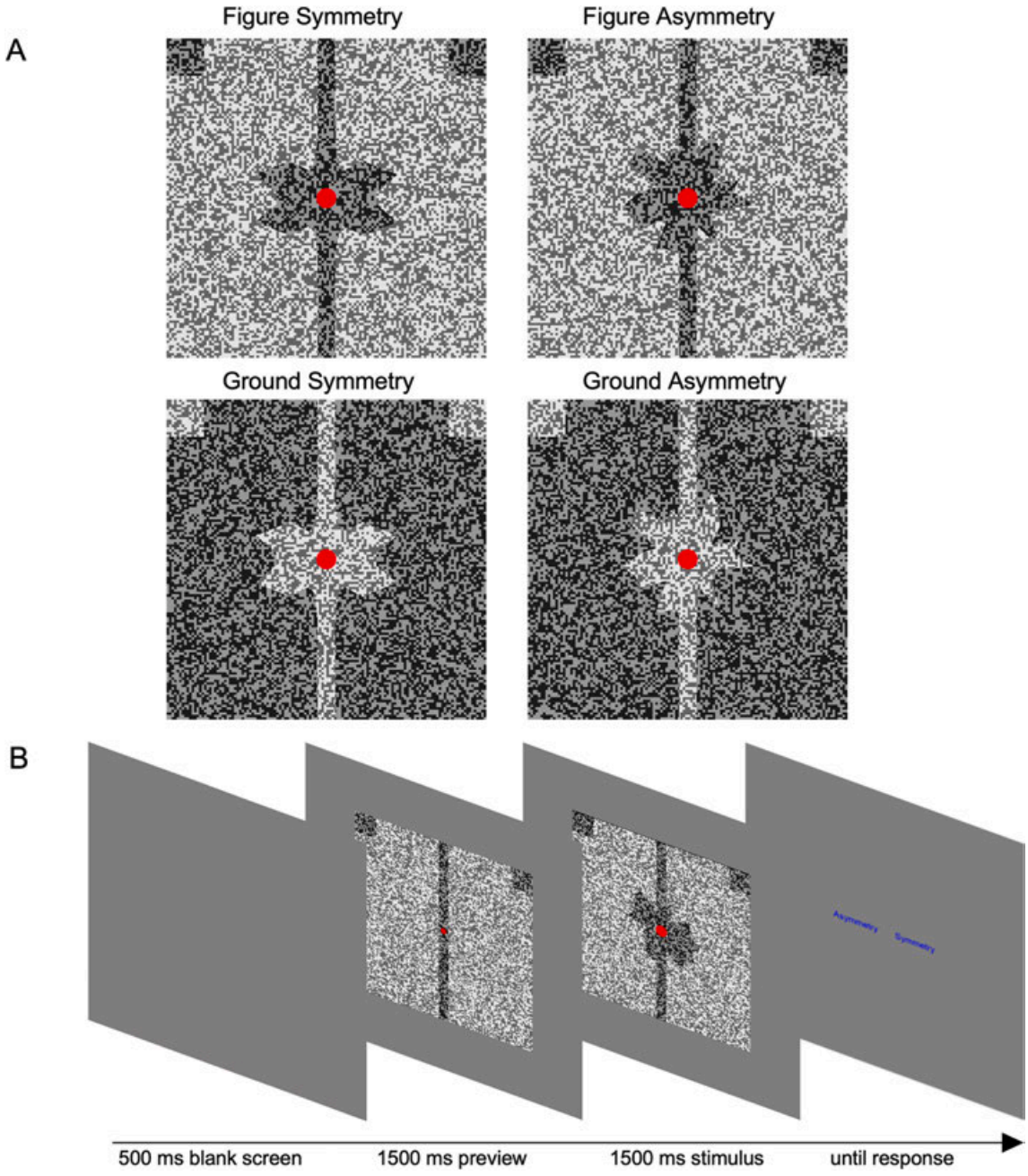

Fig. 4. Stimuli and procedure for Experiment 2. A) Example of stimuli in each of four conditions: Symmetry in the figure, Symmetry in the ground, Asymmetry in the figure, Asymmetry in the ground. The foreground region is darker for illustration. There was no brightness difference in the actual stimuli and therefore the shape could only be seen after fusion. In the experiment no polygonal shape was repeated in different trials. B) The sequence of images presented during a trial included a preview, a stimulus, and a response screen.

7. Experiment 2 method

7.1. Participants

Twenty-eight participants took part in Experiment 2 (age 18–36, mean age = 21.1, 11 male, 1 left-handed). Their stereo acuity was measured using the TNO test and it was between 15 and 120 arcsec.

7.2. Stimuli

In *Experiment 2*, two depth planes were used, one with zero disparity and one with crossed disparity to bring one surface nearer in depth. The surface in front had a disparity of 0.09°, and the background region had zero disparity. To make the surfaces visible in Fig. 4 we have decreased the luminance of the front plane. Stereograms are shown in Fig. 5. The luminance of each square was chosen at random between 22.0 cd/m^2 to 125 cd/m^2 giving an average luminance value of from 73.5 cd/m^2 on our monitor and contrast visibility of 0.70. Background grey was set at 35 cd/m^2. To minimise the delay necessary to fuse the two images, each stimulus was preceded by a preview. The preview included a vertical region that was either a figure or a ground, matched to the conditions in the experiment, as illustrated in Fig. 4B. This stimulus changed by the addition of a more complex polygon at stimulus onset. To minimise the luminance change at stimulus onset, only 50% of the squares changed luminance from preview to stimulus (randomly selected). This was the case for both planes. As in *Experiment 1*, there was a red fixation dot (radius 0.22°) in the centre of the stimulus. The radius increased to 0.43° when the stimulus was presented. This manipulation was designed to help participants maintain fixation.

In half of the trials the stimulus was an irregular polygon. In the other half it had vertical and horizontal reflectional symmetry. The polygons were generated the same way as in *Experiment 1*. Two squares (1.59° × 1.59°) were removed from the top left and top right corners of the stimuli in the ground condition, to avoid the two outside shapes having their own horizontal axis of symmetry. In the figure condition, two squares were added (1.59° × 1.59°) (see Fig. 4).

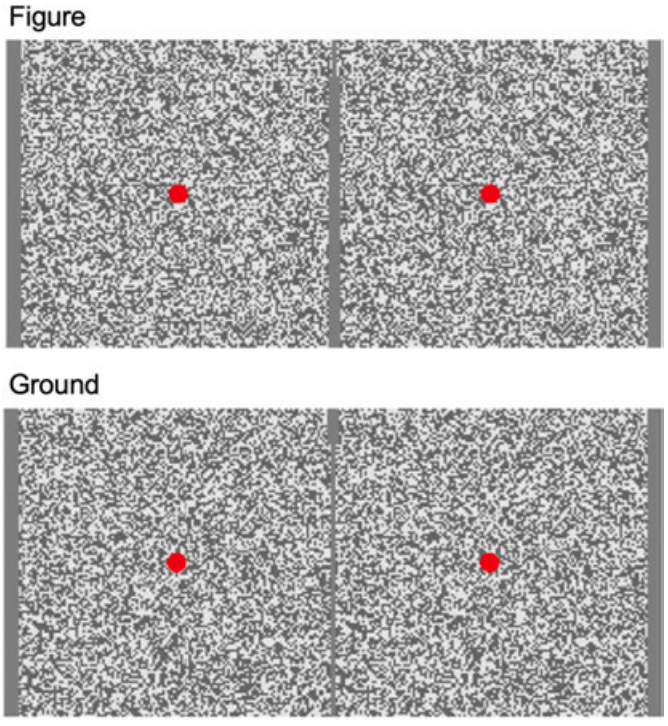

Fig. 5. Example of random dot stereograms for Experiment 2. The left image is for the left eye and the right image for the right eye. Both examples are symmetrical. The disparity was increased to 0.23° in the examples to improve visibility of the shapes.

7.3. Procedure

The procedure was similar to that of *Experiment 1*. However, in *Experiment 2* each trial began with a 1.5 s preview that included a red fixation dot (0.22°) in the middle. This was followed by a 1.5 s presentation of the stimulus (see Fig. 4B). When the stimulus was presented, there was also a 50% (0.43°) expansion of the fixation dot. After the stimulus disappeared, participants entered their responses with unpredictable key mapping. This experiment consisted of 480 trials, split into 24 blocks. Thus, there were 120 trials in each condition [Symmetry (Symmetrical, Asymmetrical) X Figure-ground (Figure, Ground) X Response screen (Left, Right)]. The conditions were fully interleaved in each block and presented in a different randomised order for each participant.

7.4. ERP analysis

Pre-processing of the data was conducted in the same way as in *Experiment 1*. In this experiment an average of 12.25 components were removed from each participant (min = 0, max = 21). Trials where participants entered the incorrect response and where the amplitude exceeded ±100 μv were excluded. The overall exclusion rate was 14.17% (6.73% errors) for figure condition and 22.14% (15.27% errors) for ground condition. SPN was defined *a-priori* as the amplitude difference between symmetrical and asymmetrical conditions at the posterior electrode cluster [PO7 O1 O2 PO8] from 400 to 1500 ms post stimulus onset (as in *Experiment 1*). After observing the ERPs, it was decided to analyse the SPN in two separate time windows, Early (400–750 ms) and Late (750–1500 ms).

8. Experiment 2 results and discussion

8.1. P1 and N1 analysis

Fig. 6A shows grand average ERP waves in each condition. The P1 was the same across conditions, but there were differences for N1. To explore these effects statistically, we obtained P1 and N1 extreme peak amplitude during the 100–180 ms and 180–400 ms windows, respectively. These effects were examined with a mixed 2 × 2 × 2 ANOVA [2 Figure-ground (Figure, Ground) X 2 Regularity (Symmetry, Asymmetry) X 2 Hemisphere (Left, Right)] for P1 and N1 separately.

For P1, there was only a significant effect of Figure-ground ($F(1,27) = 5.08$, $p = .032$, $\eta_p^2 = 0.158$). Amplitude was higher in the figure condition (mean = 2.16, SD = 1.50) compared to the ground condition (mean = 1.88, SD = 1.20).

For N1, there was no main effect of Regularity ($F(1,27) < 0.01$, $p = .999$, $\eta_p^2 < 0.001$). However, there was a significant main effect of Hemisphere ($F(1,27) = 9.21$, $p = .005$, $\eta_p^2 = 0.254$). Amplitude was more negative in the right (mean = −5.83 μv, SD = 2.72) compared to the left hemisphere (mean = −4.58 μv, SD = 2.35). N1 amplitude was also affected by Figure-ground manipulation ($F(1,27) = 6.58$, $p = .016$, $\eta_p^2 = 0.196$). N1 was larger in the Ground condition (mean = −5.55 μv, SD = 2.55) compared to the Figure condition (mean = −4.87 μv, SD = 2.46). This difference was larger in the right hemisphere. However, the interaction was non-significant.

These results are consistent with the literature. For example, Makin et al. (2014) showed N1 sensitivity to object manipulation. In Makin et al. (2014), the ground configuration involves a larger foreground area (more dots in the foreground), and that is likely to generate a larger N1. N1 may represent the orienting of attention to a task-relevant stimulus (Casco et al., 2005). Luck et al. (1990) showed that N1 attention effect was reduced when the preceding stimulus contained elements in the attended field. This might explain the smaller N1 amplitude in the figure

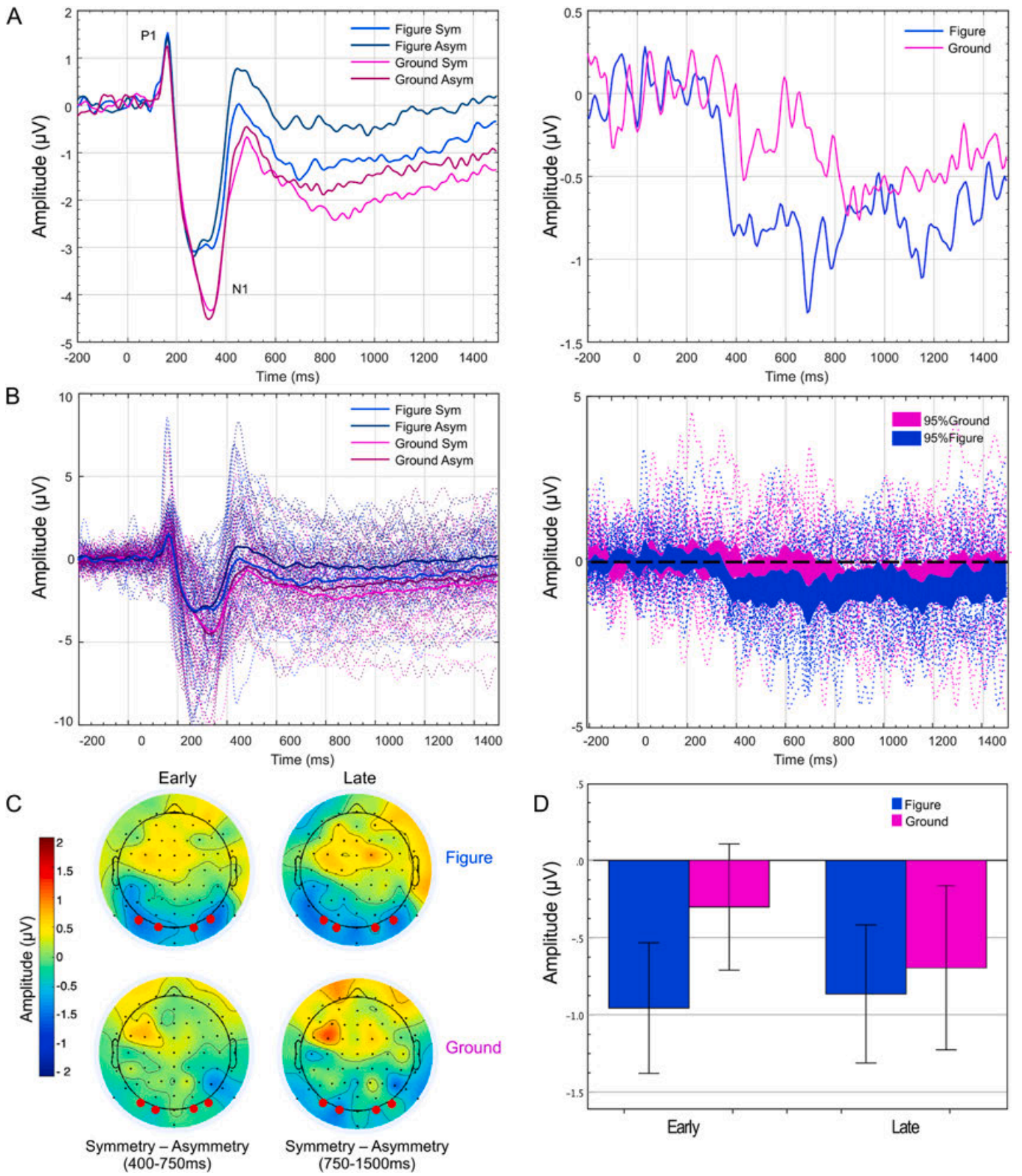

Fig. 6. A) Grand average ERPs and SPN difference waves: Waves were taken from bilateral posterior electrode cluster [PO7 O1 O2 PO8] annotated in B. The first plot shows the average ERPs, and the second plot shows the SPN as a difference from the asymmetry wave**. B) Inter-subject Variability.** The first plot shows individual-subject ERPs behind grand averages. The second plot shows 95% CI around the SPN as well as individual-subject SPNs. When the coloured ribbons do not cross zero, the SPN is significant. **C) Topographic difference maps**: These illustrate the difference between symmetrical and asymmetrical maps in Early (400–750 ms) and Late (750–1500 ms) time intervals for figure and ground. Here the SPN appears as blue at posterior electrodes. **D) SPN amplitude:** Bars show difference from asymmetry (400–1500 ms) in figure and ground split by interval (early and late). Error bars = 95% confidence intervals. The fact that error bars do not cross zero indicates the presence of a significant SPN. (For interpretation of the references to colour in this figure legend, the reader is referred to the Web version of this article.)

condition since the change, in terms of surface from preview to stimuli was smaller compared to the ground condition.

8.2. SPN analysis

The SPN is defined as the difference from the asymmetry wave, in the 400–1500 ms interval, as in Experiment 1. Behavioural filtering of the data revealed that on average participants responded correctly to 93.08% of trials in the Figure condition and 85.09% of trials in the Ground condition. A score above 75% correct responses was a condition for inclusion in the analysis, which all 28 participants satisfied.

Fig. 6 suggests SPN onset is delayed in the Ground condition. As no previous research has recorded a delay in SPN onset, we split analysis by time Window: Early (400–750 ms) and Late (750–1500 ms). SPN amplitude was then examined with 2 × 2 × 2 ANOVA [2 Figure-ground (Figure, Ground) X 2 Hemisphere (Left, Right) X 2 Interval (Early, Late)]. There was no main effect of Figure-ground ($F(1, 27) = 3.16$, $p = .087$, $\eta_p^2 = 0.105$). There was no main effect of Hemisphere ($F(1, 27) = 1.38$, $p = .250$, $\eta_p^2 = 0.049$). However, there was a significant interaction between Interval and Figure-ground ($F(1, 27) = 4.81$, $p = .037$, $\eta_p^2 = 0.151$). In the Early interval the SPN was significantly larger in the Figure condition (mean = −0.86 μV, SD = 0.96) compared to the Ground condition (mean = - 0.24 μV, SD = 0.99) ($t(27) = -2.31$, $p = .029$, $dz = -0.44$). This difference between conditions was not apparent in the Late interval (mean (Figure) = - 0.75 μV, SD = 1.04, mean (Ground) = - 0.48 μV, SD = 1.08, $t(27) = -1.05$, $p = .301$, $dz = -0.20$).

This interaction can also be demonstrated by testing whether SPN amplitude is significantly below than zero (see 95% CI in Fig. 6B and D). In the Early interval (400–750 ms) the SPN was significant for Figure ($t(27) = -4.72$, $p < .001$, $dz = -0.89$) but not for Ground ($t(27) = -1.31$, $p = .203$, $dz = -0.25$). Conversely, in the Late interval (750–1500 ms) the SPN was significant for both Figure ($t(27) = -3.79$, $p = .001$, $dz = -0.72$) and Ground ($t(27) = -2.34$, $p = .027$, $dz = -0.44$).

8.3. Explanations for SPN delay in the ground condition

Our analysis of early and late windows provides some support for an interaction between symmetry and objecthood. Symmetrical shapes tend to be seen as figures, so when symmetry is a property of a gap between objects, it creates a conflict. This delay in SPN onset may be due to object information interfering with the processing of shape information in the ground region.

One possibility is that stereo fusion was delayed in the ground condition, and this caused the SPN delay. We cannot rule this out completely, but we believe that it is unlikely. This possibility can be addressed indirectly be comparing P1 amplitude across Experiments 1 and 2. Specifically, we compared P1 from the binocular condition of Experiment 1 and the Figure condition of Experiment 2 because in these two cases the stimuli are the same. In Experiment 1 there was no preview, so stimulus onset involved the appearance of a large foreground object. This large change would generate a large P1. In Experiment 2 figure condition, the difference was the presence of a preview with a central vertical strip. Stereo fusion had already occurred before stimulus onset, and stimulus onset only involved a small increase in object surface area around fixation (Fig. 4). This small change in shape would generate a small P1. P1 amplitude was far higher in binocular condition of Experiment 1 (mean = 4.25, SD = 3.56) than in the Figure condition of Experiment 2 (mean = 1.72, SD = 1.20, $t(33.082) = 3.550$, $p = .001$, equal variance not assumed). Crucially, this suggests that the preview manipulation was successful in facilitating fusion, and that stereo fusion had already occurred at stimulus onset in Experiment 2. We thus think it is less likely stereo fusion delays are responsible for SPN delays.

The sign of the disparity was confounded with figure-ground manipulation. In the figure condition, the central stimulus had crossed disparity (near plane), in the ground condition the central stimulus had zero disparity. Other stimuli are possible. Here we focus only on one key claim: the SPN can be generated even when the symmetrical region is a ground region, and thus a region that has no ownership of the contour. In our stimuli (ground condition) the regions that do own the contours are not themselves symmetrical. Symmetry is therefore not associated with an object in this case.

8.4. Time course analysis

Experiment 2 found a novel SPN latency modulation, and this was examined indirectly, by comparing amplitude in early and late windows. We therefore decided to analyse the latency of SPN onset directly using a jackknife-based method (Miller et al., 1998). Onset estimates were retrieved using the procedure described in Smulders (2010). This was implemented using the protocol outlined by Liesefeld (2018). The procedure estimated SPN onset somewhere in 200–1500 ms interval for each participant and condition. Onset latency was defined as the time-point when the component has reached 20% of its peak amplitude.

As shown in Fig. 7A, average onset for the Figure condition was 337 ms (SD = 95) and average onset for the Ground condition was 672 ms (SD = 224). These estimates are consistent with our selection of 400 ms for the Early and 750 ms for the Late time windows.

Next, onset estimates obtained from the jackknife method were analysed statistically. A repeated measures ANOVA [Figure-Ground X Hemisphere] confirmed that onset was later in the Ground condition ($F(1,27) = 10.48$, $p = .003$, $\eta_p^2 = 0.280$). Onset was similar in both Hemispheres ($F(1,27) = 0.01$, $p = .941$, $\eta_p^2 = < 0.001$) and there was no Figure-Ground by Hemisphere interaction ($F(1,27) = 0.08$, $p = .078$, $\eta_p^2 = 0.003$). This latency analysis is more systematic than the initial amplitude analysis and uses established criteria for onset estimation. This increases confidence that the apparent SPN delay in the ground condition is not a false positive.

Scrutiny of Fig. 6A gives two impressions that require further comment. The N1 and P2 peaks appear delayed by approximately 50 ms in the Ground condition, and there is a −0.31 μV dip between 400 and 600 ms in the Ground condition difference wave. If this dip is taken as SPN onset, then our claims that the SPN is uniquely delayed in the Ground condition would not be tenable. However, there is no evidence that this 400–600 ms dip should be considered signal rather than noise. Analysis of the 450–550 ms window shows no significant effect ($t(27) -1.464$, $p = .155$, $d = 0.277$). Furthermore, confidence intervals in Fig. 6B only reveal a persistent effect after 800 ms in the Ground condition (pink ribbon). Conversely, the wave remained significantly below zero from around 400 ms onwards in the Figure condition (blue ribbon). Overall, the several converging analyses suggest SPN onset is substantially delayed in the Ground condition.

8.5. General discussion

In this study we analysed ERPs recorded when participants viewed symmetrical or asymmetrical shapes defined within random dot stereograms as surfaces separated in depth. In Experiment 1 we compared binocular and monocular cues. In Experiment 2 we compared two configurations in which the same region was presented as foreground or background. Experiment 1 confirmed the same SPN for stimuli with binocular, monocular and combined information. Previous ERP experiments have shown that suprathreshold colour and luminance signals produce the same neural response to symmetry (Martinovic et al., 2018). Our results extend these findings, showing that stereoscopic depth signals are just as efficient as monocular signals. This suggests that symmetry perception mechanisms operate at a level that is insensitive to such differences, in higher stages of visual processing. This is consistent with other work showing that the symmetry response is indifferent to the visual channels that carry element position information: for instance, the symmetry response does not distinguish between black and white elements (Makin et al., 2021).

In Experiment 2, we manipulated the figure-ground status of the

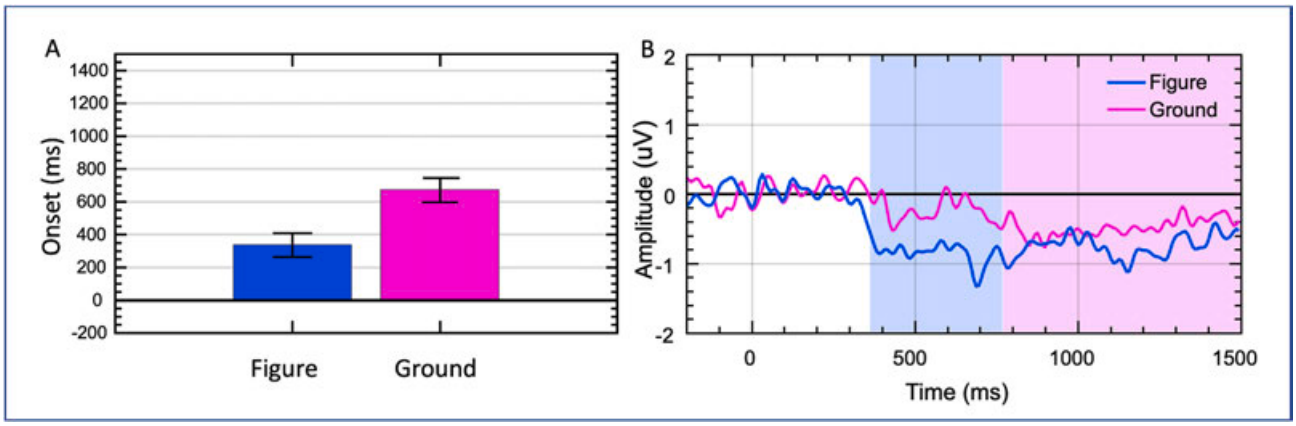

Fig. 7. A) Mean onset of SPN activity across subjects using an amplitude threshold of 20%. Error bars indicate 95% within-subjects confidence intervals. **B)** Onset of the SPN wave calculated using the grand average ERP. An amplitude threshold of 20% of the peak amplitude between 400 ms and 1000 ms was used.

symmetrical regions. Identical regions were presented, which could be symmetrical or asymmetrical, and in one condition this region was a foreground, and in the other condition it was background. As shape information becomes available only after fusion, we can be sure we are comparing conditions with different depth stratification (Bertamini and Farrant, 2006). We found that the amplitude of the SPN was not significantly affected by the figure-ground manipulation, however the onset of the SPN was delayed when symmetry was the property of the ground. In future work, different combinations of monocular and binocular depth cues could be manipulated. If multiple congruent cues support depth stratification, then the latency difference between the figure and ground conditions might be reduced or eliminated.

In psychophysical research, bilateral symmetry is most salient when it is a property of a single object (Baylis and Driver, 1995; Bertamini et al., 1997; Treder and van der Helm, 2007). Because the SPN scales with perceptual salience (Makin et al., 2016) it should be stronger when symmetry is the property of a single object. Our findings somewhat support this, as the SPN signal had a delayed onset when symmetrical contours were between two objects. Previous work has addressed effects of objectness on the EEG response to symmetry. Makin et al. (2014) found no interaction between type of symmetry and objectness on the SPN amplitude. However, in that study, contour closure supported objecthood, and this cue might not have been as strong as our disparity-defined figure and ground regions.

The SPN delay is in line with theoretical work proposing that symmetry is useful for shape detection and object recognition. Based on its ubiquity as an object property, symmetry can help to establish an *object-centred coordinate frame*, and aid object recognition (Barlow and Reeves, 1979). Studies investigating how observers construct a general, object-centred representation of an object from a viewer-centred representation have concluded that one of the critical steps is to determine the axis orientation of the object (Marr and Nishihara, 1978). Symmetry was found to be a clue to the coordinate system of the object. There is a bidirectional link between objecthood and symmetry: Objecthood aids symmetry discrimination and symmetry aids object identification. It is no surprise that symmetry and objecthood congruence effects are found at the neural level.

Processing of binocular disparity is widespread throughout the cortex, highlighting its importance for perception (Preston et al., 2008; Tsao et al., 2003). Extrastriate areas, particularly area V3a (Backus et al., 2001) and the LO (lateral occipital area) show remarkable sensitivity to stereoscopic stimuli (Preston et al., 2008). The LO activations show preferential disparity selectivity, suggesting encoding of perceptually relevant information, in contrast to activations in early visual areas (Preston et al., 2008). Imaging evidence also indirectly supports the idea that symmetry interacts with object detection. fMRI results show that visual symmetry selectively activates extrastriate areas including V3a, V4 and the LOC (Keefe et al., 2018; Sasaki et al., 2005; Tyler et al., 2005), regions that are also sensitive to object formation (Desimone, 1991; Kourtzi and Kanwisher, 2000; Pasupathy and Connor, 2002). Indeed, the LOC is functionally defined as a shape-selective area that integrates different perceptual organisation principles (Grill-Spector, 2003; Treder and van der Helm, 2007). It is possible that the LOC response to symmetry is delayed when object and symmetry cues are incongruent.

The delay in SPN for the ground condition may have emerged as an indirect consequence of conflictual information about figure-ground. This is still consistent with an association between symmetry and objecthood, but it suggests that when other cues such as size, closure and convexity are inconsistent with binocular disparity, information about the presence of an object, processing of symmetry for that object is also delayed.

These results speak to a broader question. Do different perceptual operations causally affect each other, so that the outcome of one perceptual operation alters the outcome of another? This is a question about the interdependence of perceptual operations, discussed by Hochberg (2003), Szlyk et al. (1995) and others. In our case, the first perceptual operation uses disparity cues to determine whether the central region is a foreground object. A second perceptual operation determines whether contours are mirror symmetric. These two perceptual operations are interdependent: Symmetry discrimination may be facilitated when contours are owned by one foreground object. However, our Experiment 2 shows that ownership by a single object is not a necessary condition for the presence of the SPN. This just one example of perceptual interdependence that can be fruitfully studied with ERP in future studies.

The focus of this study was the SPN, but we can also briefly comment on for N1. N1 is sensitive to stereoscopic depth information, as shown by previous research (Oliver et al., 2018). Experiment 2 found that N1 was also sensitive to figure-ground manipulation, with enhanced N1 when shapes were in the background. However, this may have been due to the larger overall area. Furthermore, N1 was right lateralized, and although we did not predict this, it is consistent with the right hemisphere dominance for many visual operations. Unlike the N1, the SPN was not significantly right lateralized here. However, symmetry processing is often stronger in the right hemisphere (Van Meel et al., 2019; Bona et al., 2015), and the SPN is right lateralized when pooling data across multiple experiments (Bertamini et al., 2018).

9. Conclusion

We found a symmetry-specific response (SPN) for shapes defined by binocular disparity within random-dot stereograms. The SPN did not differ in either latency or amplitude for binocular or monocular cues.

This suggests that symmetry sensitive networks engage mechanisms that process shape independently of the source of information. In a second study, we compared foreground and background regions. Previous psychophysical work indicated a link between bilateral symmetry and objectness. The SPN was delayed when symmetry is formed by a gap between two objects (a region of background). This may be because object formation may interfere with the processing of shape information in the ground region.

Author contributions

Elena Karakashevska co-designed and programmed the experiment, collected and analysed EEG data and wrote the manuscript. Giulia Rampone was involved in EEG data collection and analysis and writing of the manuscript. John Tyson-Carr facilitated data collection and analysis of results. Alexis Makin contributed to study design, data analysis and writing of the manuscript. Marco Bertamini generated the original idea, co-designed and programmed the experiment, contributed to interpretation of the results and wrote the manuscript.

Data sharing

All ERP and behavioural data along with the Matlab scripts are available on Open Science Framework: https://osf.io/zv5t2/.

Acknowledgements

This project was part funded by an ESRC Grant (ES/S014691/1) and by a ESRC Doctoral Training studentship (EK).

References

Backus, B.T., Fleet, D.J., Parker, A.J., Heeger, D.J., 2001. Human cortical activity correlates with stereoscopic depth perception. J. Neurophysiol. 86 (4), 2054–2068. https://doi.org/10.1152/jn.2001.86.4.2054.

Bahnsen, P., 1928. Eine Untersuchung über Symmetrie und Asymmetrie bei visuellen Wahrnehmungen. Z. für Psychol. 108, 129–154.

Barlow, H.B., Reeves, B.C., 1979. The versatility and absolute efficiency of detecting mirror symmetry in random dot displays. Vis. Res. 19 (7), 783–793. https://doi.org/10.1016/0042-6989(79)90154-8.

Baylis, G.C., Driver, J., 1995. One-sided edge assignment in vision: 1. Figure-ground segmentation and attention to objects. Curr. Dir. Psychol. Sci. 4 (5), 140–146. https://doi.org/10.1111/1467-8721.ep10772580.

Bertamini, M., Farrant, T., 2006. The perceived structural shape of thin (wire-like) objects is different from that of silhouettes. Perception 35 (12), 1679–1692. https://doi.org/10.1068/p5534.

Bertamini, M., Makin, A., 2014. Brain activity in response to visual symmetry. Symmetry 6 (4), 975–996. https://doi.org/10.3390/sym6040975.

Bertamini, M., Friedenberg, J.D., Kubovy, M., 1997. Detection of symmetry and perceptual organization: the way a lock-and-key process works. Acta Psychol. 95 (2), 119–140. https://doi.org/10.1016/S0001-6918(96)00038-8.

Bertamini, M., Friedenberg, J., Argyle, L., 2002. No within-object advantage for detection of rotation. Acta Psychol. 111 (1), 59–81. https://doi.org/10.1016/S0001-6918(02)00043-4.

Bertamini, M., Silvanto, J., Norcia, A.M., Makin, A.D.J., Wagemans, J., 2018. The neural basis of visual symmetry and its role in mid- and high-level visual processing: neural basis of visual symmetry. Ann. N. Y. Acad. Sci. 1426 (1), 111–126. https://doi.org/10.1111/nyas.13667.

Bona, S., Cattaneo, Z., Silvanto, J., 2015. The causal role of the occipital face area (OFA) and lateral occipital (LO) cortex in symmetry perception. J. Neurosci. 35 (2), 731–738. https://doi.org/10.1523/JNEUROSCI.3733-14.2015.

Carmody, D.P., Nodine, C.F., Locher, P.J., 1977. Global detection of symmetry. Percept. Mot. Skills 45 (3_Suppl. l), 1267–1273. https://doi.org/10.2466/pms.1977.45.3f.1267.

Casco, C., Grieco, A., Campana, G., Corvino, M.P., Caputo, G., 2005. Attention modulates psychophysical and electrophysiological response to visual texture segmentation in humans. Vis. Res. 45 (18), 2384–2396. https://doi.org/10.1016/j.visres.2005.02.022.

Cattaneo, Z., 2017. The neural basis of mirror symmetry detection: a review. J. Cognit. Psychol. 29 (3), 259–268.

Cattaneo, Z., Bona, S., Bauer, C., Silvanto, J., Herbert, A., Vecchi, T., Merabet, L., 2014. Symmetry detection in visual impairment: behavioral evidence and neural correlates. Symmetry 6 (2), 427–443. https://doi.org/10.3390/sym6020427.

Chen, C.C., Kao, K.L.C., Tyler, C.W., 2007. Face configuration processing in the human brain: the role of symmetry. Cerebr. Cortex 17, 1423–1432.

Corballis, M.C., Roldan, C.E., 1974. On the perception of symmetrical and repeated patterns. Percept. Psychophys. 16 (1), 136–142. https://doi.org/10.3758/BF03203266.

DeAngelis, G.C., Newsome, W.T., 1999. Organization of disparity-selective neurons in macaque area MT. J. Neurosci. 19 (4), 1398–1415. https://doi.org/10.1523/JNEUROSCI.19-04-01398.1999.

Delorme, A., Makeig, S., 2004. EEGLAB: an open source toolbox for analysis of single-trial EEG dynamics including independent component analysis. J. Neurosci. Methods 134 (1), 9–21. https://doi.org/10.1016/j.jneumeth.2003.10.009.

Desimone, R., 1991. Neural mechanisms of attention and memory in extrastriate cortex. Neurosci. Res. Suppl. 16, X. https://doi.org/10.1016/0921-8696(91)90621-S.

Duan, Y., Thatte, J., Yaklovleva, A., Norcia, A., 2021. Disparity in Context: understanding how monocular image content interacts with disparity processing in human visual cortex. Neuroimage 237, 118139. https://doi.org/10.1016/j.neuroimage.2021.118139.

Gilaie-Dotan, S., Ullman, S., Kushnir, T., Malach, R., 2002. Shape-selective stereo processing in human object-related visual areas. Hum. Brain Mapp. 15 (2), 67–79. https://doi.org/10.1002/hbm.10008.

Grill-Spector, K., 2003. The neural basis of object perception. Curr. Opin. Neurobiol. 13 (3), 399. https://doi.org/10.1016/S0959-4388(03)00060-6.

Hochberg, J., 2003. Acts of perceptual inquiry: problems for any stimulus-based simplicity theory. Acta Psychol. 114 (3), 215–228.

Höfel, L., Jacobsen, T., 2007. Electrophysiological indices of processing aesthetics: spontaneous or intentional processes? Int. J. Psychophysiol. 65 (1), 20–31. https://doi.org/10.1016/j.ijpsycho.2007.02.007.

Jacobsen, T., Höfel, L., 2003. Descriptive and evaluative judgment processes: behavioral and electrophysiological indices of processing symmetry and aesthetics. Cognit. Affect Behav. Neurosci. 3 (4), 289–299. https://doi.org/10.3758/CABN.3.4.289.

Julesz, B., 1986. Stereoscopic vision. Vis. Res. 26 (9), 1601–1612. https://doi.org/10.1016/0042-6989(86)90178-1.

Jung, T.P., Makeig, S., Humphries, C., Lee, T.W., McKeown, M.J., Iragui, V., et al., 2000. Removing electroencephalographic artifacts by blind source separation. Psychophysiology 37, 163–178.

Kanizsa, G., Gerbino, W., 1976. Convexity and symmetry in figure-ground organization. In: Vision and Artifact. Springer, New York, pp. 25–32.

Keefe, B.D., Gouws, A.D., Sheldon, A.A., Vernon, R.J.W., Lawrence, S.J.D., McKeefry, D. J., Wade, A.R., Morland, A.B., 2018. Emergence of symmetry selectivity in the visual areas of the human brain: FMRI responses to symmetry presented in both frontoparallel and slanted planes. Hum. Brain Mapp. 39 (10), 3813–3826. https://doi.org/10.1002/hbm.24211.

Kohler, P.J., Clarke, A., Yakovleva, A., Liu, Y., Norcia, A.M., 2016. Representation of maximally regular textures in human visual cortex. J. Neurosci. 36 (3), 714–729. https://doi.org/10.1523/JNEUROSCI.2962-15.2016.

Koning, A., Wagemans, J., 2009. Detection of symmetry and repetition in one and two objects: structures versus strategies. Exp. Psychol. 56 (1), 5–17. https://doi.org/10.1027/1618-3169.56.1.5.

Kourtzi, Z., Kanwisher, N., 2000. Cortical regions involved in perceiving object shape. J. Neurosci. 20 (9), 3310–3318 https://doi.org/10/gfrjgp.

Liesefeld, H.R., 2018. Estimating the timing of cognitive operations with MEG/EEG latency measures: a primer, a brief tutorial, and an implementation of various methods. Front. Neurosci. 12, 765. https://doi.org/10.3389/fnins.2018.00765.

Little, A.C., Jones, B.C., DeBruine, L.M., 2011. Facial attractiveness: evolutionary based research. Phil. Trans. Biol. Sci. 366 (1571), 1638–1659. https://doi.org/10.1098/rstb.2010.0404.

Livingstone, M., Hubel, D., 1988. Segregation of form, color, movement, and depth: anatomy, physiology, and perception. Science 240 (4853), 740–749. https://doi.org/10.1126/science.3283936.

Luck, S.J., Heinze, H.J., Mangun, G.R., Hillyard, S.A., 1990. Visual event-related potentials index focused attention within bilateral stimulus arrays. II. Functional dissociation of P1 and N1 components. Electroencephalogr. Clin. Neurophysiol. 75 (6), 528–542. https://doi.org/10.1016/0013-4694(90)90139-B.

Mach, E, 1897. The Analysis of Sensations. Open Court Publishing House., Chicago.

Machilsen, B., Pauwels, M., Wagemans, J., 2009. The role of vertical mirror symmetry in visual shape detection. J. Vis. 9 (12), 11. https://doi.org/10.1167/9.12.11, 11.

Makin, A.D.J., Pecchinenda, A., Bertamini, M., 2012a. Grouping by closure influences subjective regularity and implicit preference. I-Perception 3 (8), 519–527. https://doi.org/10.1068/i0538.

Makin, A.D.J., Piovesan, A., Tyson-Carr, J., Rampone, G., Derpsch, Y., Bertamini, M., 2021. Electrophysiological priming effects confirm that the extrastriate symmetry network is not gated by luminance polarity. Eur. J. Neurosci. 53 (4), 964–973. https://doi.org/10.1111/ejn.14966.

Makin, A.D.J., Rampone, G., Bertamini, M., 2015. Conditions for view invariance in the neural response to visual symmetry: view invariance and symmetry ERPs. Psychophysiology 52 (4), 532–543. https://doi.org/10.1111/psyp.12365.

Makin, A.D.J., Rampone, G., Morris, A., Bertamini, M., 2020. The formation of symmetrical gestalts is task-independent but can Be enhanced by active regularity discrimination. J. Cognit. Neurosci. 32 (2), 353–366. https://doi.org/10.1162/jocn_a_01485.

Makin, A.D.J., Rampone, G., Pecchinenda, A., Bertamini, M., 2013. Electrophysiological responses to visuospatial regularity: electrophysiological responses to visuospatial regularity. Psychophysiology 25, 376–385. https://doi.org/10.1111/psyp.12082.

Makin, A.D.J., Rampone, G., Wright, A., Martinovic, J., Bertamini, M., 2014. Visual symmetry in objects and gaps. J. Vis. 14 (3), 12. https://doi.org/10.1167/14.3.12.

Makin, A.D.J., Wilton, M.M., Pecchinenda, A., Bertamini, M., 2012b. Symmetry perception and affective responses: a combined EEG/EMG study. Neuropsychologia 50 (14), 3250–3261. https://doi.org/10.1016/j.neuropsychologia.2012.10.003.

Makin, A.D.J., Wright, D., Rampone, G., Palumbo, L., Guest, M., Sheehan, R., Cleaver, H., Bertamini, M., 2016. An electrophysiological index of perceptual goodness. Cerebr. Cortex 26 (12), 4416–4434. https://doi.org/10.1093/cercor/bhw255.

Marr, D., Nishihara, H.K., 1978. Representation and recognition of the spatial organization of three-dimensional shapes. Proc. Roy. Soc. Lond. B Biol. Sci. 200 (1140), 269–294. https://doi.org/10.1098/rspb.1978.0020.

Martinovic, J., Jennings, B.J., Makin, A.D.J., Bertamini, M., Angelescu, I., 2018. Symmetry perception for patterns defined by color and luminance. J. Vis. 18 (8), 4. https://doi.org/10.1167/18.8.4.

Miller, J., Patterson, T., Ulrich, R., 1998. Jackknife-based method for measuring LRP onset latency differences. Psychophysiology 35 (1), 99–115. https://doi.org/10.1111/1469-8986.3510099.

Mojica, A.J., Peterson, M.A., 2014. Display-wide influences on figure–ground perception: the case of symmetry. Atten. Percept. Psychophys. 76 (4), 1069–1084. https://doi.org/10.3758/s13414-014-0646-y.

Masson, M.E., 2011. A tutorial on a practical Bayesian alternative to null-hypothesis significance testing. Behav. Res. Methods 43 (3), 679–690. https://doi.org/10.3758/s13428-010-0049-5.

Neri, P., 2005. A stereoscopic look at visual cortex. J. Neurophysiol. 93 (4), 1823–1826.

Norcia, A.M., Candy, T.R., Pettet, M.W., Vildavski, V.Y., Tyler, C.W., 2002. Temporal dynamics of the human response to symmetry. J. Vis. 2 (2) https://doi.org/10.1167/2.2.1.

Oliver, Z.J., Cristino, F., Roberts, M.V., Pegna, A.J., Leek, E.C., 2018. Stereo viewing modulates three-dimensional shape processing during object recognition: a high-density ERP study. J. Exp. Psychol. Hum. Percept. Perform. 44 (4), 518–534. https://doi.org/10.1037/xhp0000444.

Orban, G., Janssen, P., Vogels, R., 2006. Extracting 3D structure from disparity. Trends Neurosci. 29 (8), 466–473. https://doi.org/10.1016/j.tins.2006.06.012.

Palumbo, L., Bertamini, M., Makin, A., 2015. Scaling of the extrastriate neural response to symmetry. Vis. Res. 117, 1–8. https://doi.org/10.1016/j.visres.2015.10.002.

Parker, A.J., 2007. Binocular depth perception and the cerebral cortex. Nat. Rev. Neurosci. 8 (5), 379–391.

Pasupathy, A., Connor, C.E., 2002. Population coding of shape in area V4. Nat. Neurosci. 5 (12), 1332–1338. https://doi.org/10.1038/972.

Pegna, A.J., Darque, A., Roberts, M.V., Leek, E.C., 2018. Effects of stereoscopic disparity on early ERP components during classification of three-dimensional objects. Q. J. Exp. Psychol. 71 (6), 1419–1430. https://doi.org/10.1080/17470218.2017.1333129.

Peirce, J.W., 2007. PsychoPy—psychophysics software in Python. J. Neurosci. Methods 162 (1–2), 8–13. https://doi.org/10.1016/j.jneumeth.2006.11.017.

Preston, T.J., Li, S., Kourtzi, Z., Welchman, A.E., 2008. Multivoxel pattern selectivity for perceptually relevant binocular disparities in the human brain. J. Neurosci. 28 (44), 11315–11327. https://doi.org/10.1523/JNEUROSCI.2728-08.2008.

Rampone, G., O' Sullivan, N., Bertamini, M., 2016. The role of visual eccentricity on preference for abstract symmetry. PLoS One 11 (4), e0154428. https://doi.org/10.1371/journal.pone.0154428.

Sasaki, Y., Vanduffel, W., Knutsen, T., Tyler, C., Tootell, R., 2005. Symmetry activates extrastriate visual cortex in human and nonhuman primates. Proc. Natl. Acad. Sci. Unit. States Am. 102 (8), 3159–3163. https://doi.org/10.1073/pnas.0500319102.

Sawada, T., Pizlo, Z., 2008. Detection of skewed symmetry. J. Vis. 8 (5), 14. https://doi.org/10.1167/8.5.14.

Smulders, F.T.Y., 2010. Simplifying jackknifing of ERPs and getting more out of it: retrieving estimates of participants' latencies. Psychophysiology 47 (2), 387–392. https://doi.org/10.1111/j.1469-8986.2009.00934.x.

Szlyk, J., Fisher, C., Rock, I., 1995. Level of processing in the perception of symmetrical forms viewed from different angles. Spatial Vis. 9 (1), 139–150.

Swaddle, J.P., 1999. Visual signalling by asymmetry: a review of perceptual processes. Phil. Trans. Roy. Soc. Lond. B Biol. Sci. 354 (1388), 1383–1393. https://doi.org/10.1098/rstb.1999.0486.

Treder, M.S., van der Helm, P.A., 2007. Symmetry versus repetition in cyclopean vision: a microgenetic analysis. Vis. Res. 47 (23), 2956–2967. https://doi.org/10.1016/j.visres.2007.07.018.

Tsao, D.Y., Vanduffel, W., Sasaki, Y., Fize, D., Knutsen, T.A., Mandeville, J.B., Wald, L.L., Dale, A.M., Rosen, B.R., Van Essen, D.C., Livingstone, M.S., Orban, G.A., Tootell, R.B. H., 2003. Stereopsis activates V3A and caudal intraparietal areas in macaques and humans. Neuron 39 (3), 555–568. https://doi.org/10.1016/S0896-6273(03)00459-8.

Tyler, C.W., Baseler, H.A., Kontsevich, L.L., Likova, L.T., Wade, A.R., Wandell, B.A., 2005. Predominantly extra-retinotopic cortical response to pattern symmetry. Neuroimage 24 (2), 306–314. https://doi.org/10.1016/j.neuroimage.2004.09.018.

Vancleef, K., Read, J.C.A., Herbert, W., Goodship, N., Woodhouse, M., Serrano-Pedraza, I., 2017. Overestimation of stereo thresholds by the TNO stereotest is not due to global stereopsis. Ophthalmic Physiol. Opt. 37 (4), 507–520.

Van Meel, C., Baeck, A., Gillebert, C.R., Wagemans, J., de Beeck, H.P.O., 2019. The representation of symmetry in multi-voxel response patterns and functional connectivity throughout the ventral visual stream. Neuroimage 191, 216–224. https://doi.org/10.1016/j.neuroimage.2019.02.030.

Wagemans, J., Elder, J.H., Kubovy, M., Palmer, S.E., Peterson, M.A., Singh, M., von der Heydt, R., 2012. A century of Gestalt psychology in visual perception: I. Perceptual grouping and figure–ground organization. Psychol. Bull. 138 (6), 1172–1217. https://doi.org/10.1037/a0029333.

Wagemans, J., Van Gool, L., D'ydewalle, G., 1991. Detection of symmetry in tachistoscopically presented dot patterns: effects of multiple axes and skewing. Percept. Psychophys. 50 (5), 413–427. https://doi.org/10.3758/BF03205058.